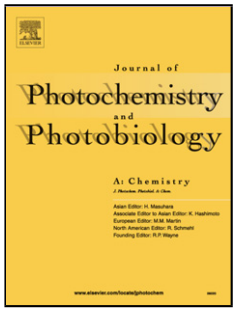

Title: Exploiting the INHIBIT-ESIPT Mechanism for the Design of Fluorescent Chemosensor with a Large Blue-Shift in Emission

Author: Gargi Dhaka Navneet Kaur Jasvinder Singh

PII: S1010-6030(16)30818-8
DOI: http://dx.doi.org/doi:10.1016/j.jphotochem.2016.11.018
Reference: JPC 10442

To appear in: *Journal of Photochemistry and Photobiology A: Chemistry*

Received date: 27-9-2016
Revised date: 11-11-2016
Accepted date: 13-11-2016

Please cite this article as: Gargi Dhaka, Navneet Kaur, Jasvinder Singh, Exploiting the INHIBIT-ESIPT Mechanism for the Design of Fluorescent Chemosensor with a Large Blue-Shift in Emission, Journal of Photochemistry and Photobiology A: Chemistry http://dx.doi.org/10.1016/j.jphotochem.2016.11.018

Exploiting the INHIBIT-ESIPT Mechanism for the Design of Fluorescent Chemosensor with a Large Blue-Shift in Emission

Gargi Dhaka, Navneet Kaur* and Jasvinder Singh

Department of Chemistry, Panjab University, Chandigarh 160014, India

∗ Corresponding author. Tel.: +91 172 2534430; fax: +91 172 2545074;
e-mail: neet_chem@yahoo.co.in; neet_chem@pu.ac.in

Graphical Abstract

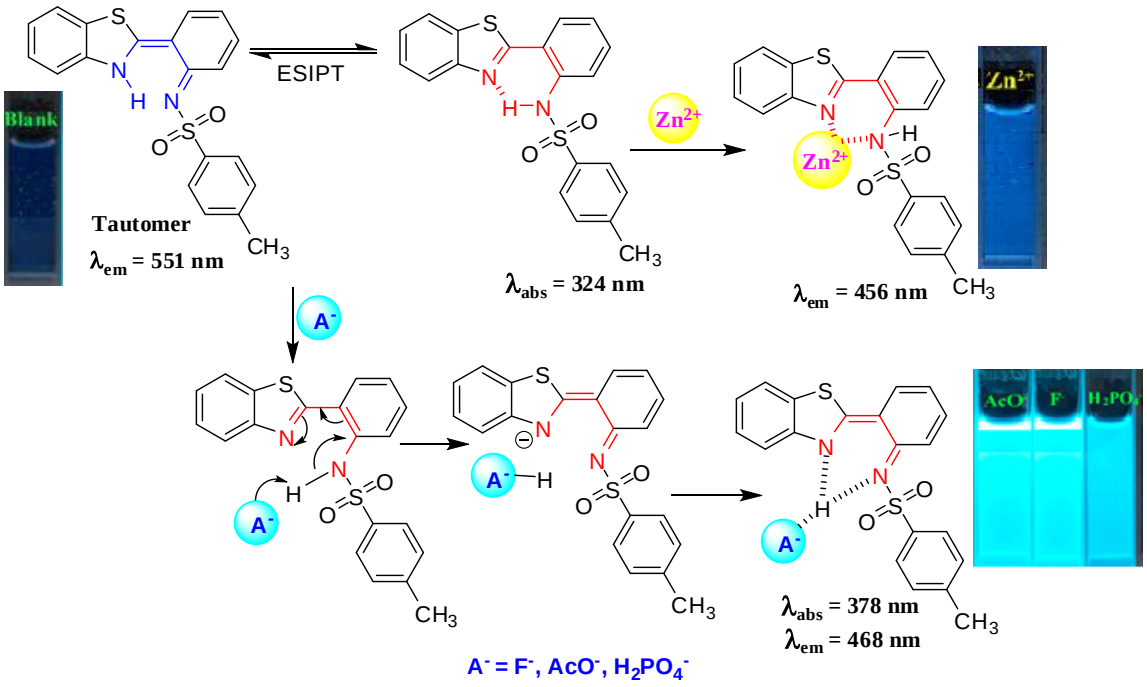

Highlights

- Benzothiazole based sulfonamide possessing chemosensopr for Zn^{2+}, F^-, AcO^- and $H_2PO_4^-$ ions.
- Anions addition resulted in formation of new band at longer wavelength ($\Delta\lambda$ = 54 nm) in UV-vis spectra
- Zn^{2+} and anions addition caused substantial blue shift ($\Delta\lambda$ = 83 nm) along with fluorescent enhancement in fluorescence spectra.
- Inhibition of ESIPT responsible for absorption and fluorescence changes.

Abstract:
A set of two novel fluoroscent receptors **2a** and **2b** with sulfonamide binding site and 2-(2'-aminophenyl)benzothiazole scaffolding as a signaling unit have been synthesized by condensation approach, which can undergo excited-state intramolecular proton transfer (ESIPT) upon excitation. In CH_3CN solution of **2a**, this ESIPT phenomenon was perturbed and showed a remarkable hypsochromic shift ($\Delta\lambda \sim 83$ nm), by capturing of Zn^{2+} metal ion selectively out of other interfering metal ions including Na^+, K^+, Mg^{2+}, Al^{3+}, Mn^{2+}, Fe^{2+}, Co^{2+}, Ni^{2+}, Cu^{2+}, Cd^{2+} and Hg^{2+}. Similarly, the deprotonation of the sulfonamide proton of this acidic receptor **2a** by basic anions such as F^-, AcO^-, and $H_2PO_4^-$ also resulted in a substantial blue shift due to disruption of ESIPT. This blue shift was accompanied by enhancement of emission intensity and fluorescent color change from dark blue to light blue.

Keywords: Benzothiazole; ESIPT; Anion sensing; Zn^{2+} sensor

1. Introduction

Currently, chemosensors that translate molecular recognition into highly sensitive and simply detected signals have been keenly investigated. Fluorescence-based probes provide high sensitivity and are therefore on the whole well suited for the visualization of cations and anions in the media contaminated with them [1]. In particular, the development of a fluorescent probe for Zn^{2+} ion in the presence of a variety of other metal ions has fetched great consideration [2-3]. These efforts are motivated by the fact that Zn^{2+} is the second most abundant transition-metal in living organisms and performing significant roles in physiological and pathological processes such as neural signal transmission, regulators of enzymes, structural cofactors in metalloproteins, and gene expression [4-5]. Amusingly, to compare with other tissues, high concentrations of Zn^{2+} are present in pancreatic islets, which act critically in insulin biosynthesis, storage, and secretion [6]. It is also reported that Zn^{2+} ion is a potent killer of neurons via oxidative stress, the cause of neurodegenerative disorders such as Alzheimer's disease (AD), amyotrophic lateral sclerosis (ALS), Guam ALS-parkinsonism dementia, Parkinson's disease, hypoxiaischemia, and epilepsy [7-8].

Likewise, there exists a great interest in the development of synthetic receptors for anions too, due to their medicinal and environment potential applications [9-10]. In particular, the carboxylate and fluoride anions are critical components of numerous metabolic processes and also exhibit specific biochemical behaviors in the enzymes and antibodies [11].

Arrays of Zn^{2+} selective fluorescent sensors employing fluorescein [12], quinolone [13], indole [14], coumarin [15] and other fluorophores [16] or proteins [17] have been developed, but a bulk of these, translates the binding event into either an increase or decrease of the emission intensity [18]. However, probes that exhibit a spectral shift upon binding to the analyte offer an elegant way out to this problem [19]. Moreover, excited-state intramolecular proton transfer (ESIPT) is a renowned photophysical process responsible for unusually large stoke shifts in benzazole. Inhibition of the ESIPT process by cation binding yields a significant hypsochromic shift of the fluorescence emission maximum [20-22]. Although inhibition of the ESIPT has been greatly exploited for cation sensing, it was scantily employed for the anion sensing [23].

To prepare an ESIPT-based chemosensor, the sensor moiety should form an intramolecular hydrogen bond in the ground state with the adjacent hydrogen-bond acceptor [24-25]. Therefore we introduced sulfonamide group of moderate acidity, as a binding moiety, which is a good hydrogen-bonding donor and can bind efficiently with both the cations and anions. However, use of heteroaromatic ring system such as thiazole, which contains soft heteroatoms N and S, as electron donors to metal cations, particularly Zn^{2+}, is very rare in literature [26]. To date, application of benzofused heteroaromatic ring system eg. benzothiazole, having substitution at 2 and 2' position, as a Zn^{2+} chemosensor based on INHIBIT-ESIPT mechanism has not been reported to the best of our knowledge.

2. Materials and Methods

All solvents and reagents were purchased from Aldrich. All other chemicals were used as received without further purification. Deionized water was used throughout the experiments. Acetonitrile (CH_3CN) was of HPLC grade. The UV-Vis spectra were recorded on a Jasco v – 530 UV/ Vis spectrophotometer. All fluorescence spectra were recorded on Hitachi F-7000 spectrophotometer. All the metal ions such as Na^+, K^+, Mg^{2+}, Mn^{2+}, Fe^{2+}, Co^{2+}, Ni^{2+}, Cu^{2+}, Zn^{2+}, Hg^{2+} and Cd^{2+} were added as their perchlorate salts; whereas all the anions such as F^-, Cl^-, Br^-, I^-, AcO^-, $H_2PO_4^-$, CN^-, HSO_4^- and SO_4^{2-} were added as their tetrabutylammonium salts for the different UV-Vis and fluorescence spectroscopic experiments.

Melting point was determined in capillary and is uncorrected. ^1H and ^{13}C NMR spectra were recorded on a BRUKER AVANCE 400 and 100 MHz instrument using tetramethylsilane as an internal standard. The chemical shifts are reported in δ values relative to TMS and coupling constants (J) are expressed in Hz. ^{13}C NMR spectra were recorded at 100 MHz and values are reported relative to $CDCl_3$ signal at δ 77.0.

2.1 General procedure for fluorescence experiments

Fluorescence spectra were recorded using HITACHI-7000 spectrophotometer with quartz cell of 1 cm width and 3.5 cm height. The excitation was carried out at 340 nm for probe **2a** and **2b** with 5 nm excitation and emission slit widths in fluorometer. Stock solution of the probe **2a** and **2b** (1 x 10^{-2} M) was prepared in DMSO. This stock solution was diluted with CH_3CN and used further for different spectroscopic experiments. All absorption scans were saved as ACS II files and further processed in Excel(tm) to produce all graphs shown.

2.2 General procedure for ^1H NMR experiments

The ^1H NMR titrations were carried out in DMSO-d_6 using TMS as an internal reference standard. To the 3.0 x 10^{-3} M solution of **2a** in DMSO, the varying equivalents of $TBA+F^-$ were added and ^1H NMR spectra were recorded after each addition.

3. Experimental

*3.1 Synthesis of 2-(Benzothiazol-2-yl)-aniline (**1**)*

Absolute ethanol was added to mixture of previously synthesized 2-(2-nitrophenyl)benzothiazole (250 mg, 1mmol) and $SnCl_2.2H_2O$ (439 mg, 5 mmol) and refluxed at 70 ^oC for 5 hrs [27]. After completion of reaction (TLC), the crude product was separated and recrystallized to yield light yellow reduced product **1**. Yellow solid, mp (^oC) 184, Yield (%) 70; IR (cm^{-1}) 3453.87 and 3284.13 (two sharp peaks, ν_{NH2}), 1603.05 ($\nu_{C=Nstr}$) 1487.55 ($\nu_{C-Nstr.}$); 1H NMR (DMSO, 400 MHz) δ (ppm): 6.32 (s, 2H, NH_2), 6.67 (t, $J_1 = J_2$ = 8.0 Hz, 1H, ArH), 6.71 (d, J = 8.0 Hz, 1H, ArH), 7.15 (t, $J_1 = J_2$ = 8.0 Hz, 1H, ArH), 7.27 (t, $J_1 = J_2$ = 8.0 Hz, 1H, ArH), 7.38 (t, $J_1 = J_2$ = 8.0 Hz, 1H, ArH), 7.63 (d, J = 8.0 Hz, 1H, ArH), 7.80 (d, J = 8.0 Hz, 1H, ArH), 7.89 (d, J = 8.0 Hz, 1H, ArH); ^{13}C NMR ($CDCl_3$, 75 MHz) δ (ppm): 169.24, 159.74, 146.78, 133.27, 131.82, 130.98, 126.04, 124.87, 122.48, 121.20, 116.91, 116.81, 115.28; ESI-MS: m/z (relative abundance (%), assignment) = 227.2 [$(M+1)^+$].

*3.2 Synthesis of N-(2-(Benzothiazol-2-ylphenyl)-4-methylbenzenesulfonamide (**2a**)*

The mixture of **1** (250 mg, 1 mmol) and 4-methylbenzenesulfonyl chloride (202 mg, 1.3 mmol) in the presence of K_2CO_3 (183 mg, 1.2 mmol) was refluxed at 80 ^0C in dry CH_3CN with a catalytic amount of salt $TBA^+HSO_4^-$. After completion of reaction (TLC), the reaction mixture was allowed to cool down and then filtered off. The filtrate was kept under high vacuum to obtain the solid compound which was further purified by recrystallisation method to yield pure **2a**. Light Brown solid, mp (^oC) 150, yield (%) 78; IR (cm^{-1}) 3648 (ν_{N-Hstr}), 3064 ($\nu_{Ar-Hstr}$), 1583 ($\nu_{C=Nstr}$), 1483 (ν_{C-Nstr}); ^1H NMR ($CDCl_3$, 400 MHz) δ (ppm): 2.24 (s, 3H, $-CH_3$), 7.19 (d, 2H, J = 8.0 Hz, ArH), 7.26 (t, 1H, $J_1 = J_2$ = 8.0 Hz, ArH), 7.37 (t, 1H, $J_1 = J_2$

= 8.0 Hz, ArH), 7.50 (t, 1H, J_1 = J_2 = 8.0 Hz, ArH), 7.55 (t, 1H, J_1 = J_2 = 8.0 Hz, ArH), 7.58 (d, 2H, *J* = 8.0 Hz, ArH), 7.63 (d, 1H, *J* = 8.0 Hz, ArH), 7.91 (d, 1H, *J* = 8.0 Hz, ArH), 8.10 (d, 1H, *J* = 8.0 Hz, ArH), 8.18 (d, 1H, *J* = 8.0 Hz, ArH), 11.8 (s, 1H, NH); ^{13}C NMR ($CDCl_3$, 100 MHz) δ (ppm): 167.9, 152.6, 143.5, 136.9, 136.6, 133.2, 131.7, 129.9, 129.4, 127.1, 126.8, 125.9, 123.7, 123.1, 121.3, 120.4, 120.3, 21.5; ESI-MS: m/z (relative abundance (%), assignment) = 381.2 [100, $(M+1)^+$].

*3.3 Synthesis of N-(-6-(Benzothiazol-2(3H)-ylidene)cyclohexa-2,4-dienylidene)-4-nitro-benzenesulfonamide (**2b**)*

The reaction of **1** with 4-nitrobenzenesulfonyl chloride in similar reaction conditions as for **2a**, yielded **2b**. Pale yellow solid, mp (^{o}C) 210, Yield (%) 79; IR (cm^{-1}) 3080 ($\nu_{Ar\text{-}Hstr}$), 1583 ($\nu_{C=Nstr}$), 1487 ($\nu_{C\text{-}Nstr}$); ^{1}H NMR (DMSO-d_6, 400 MHz) δ (ppm): 7.06 (t, 1H, J_1 = J_2 = 8.0 Hz, ArH), 7.21 (s, 1H, NH, exchanges with D_2O), 7.31 (d, 1H, *J* = 8.0 Hz, ArH), 7.35 (t, 1H, J_1 = J_2 = 8.0 Hz, ArH), 7.43 (t, 1H, J_1 = J_2 = 8.0 Hz, ArH), 7.74 (d, 1H, *J* = 8.0 Hz, ArH), 7.85 (d, 1H, *J* = 8.0 Hz, ArH), 7.93 (d, 3H, *J* = 8.0 Hz, ArH), 8.07 (d, 2H, *J* = 8.0 Hz, ArH); ^{13}C NMR ($CDCl_3$, 100 MHz) δ (ppm): 167.8, 152.9, 147.9, 139.6, 131.6, 130.1, 127.1, 126.4, 125.5, 123.7, 122.6, 121.8, 121.3, 120.5, 119.1; ESI-MS: m/z (relative abundance (%), assignment) = 492.4 [100, $(M+2)^+ + 2K^+$]. Due to poor solubility and for getting better D_2O exchange NMR, ^{1}H NMR of **2b** was carried out in DMSO-d_6.

4. Results and Discussions

Scheme 1 outlines the synthesis of sulfonamide possessing benzothiazole derivatives, **2a** and **2b**. The refluxing of **1** with different sulfonyl chloride, in dry CH_3CN, gave respective derivatives, **2a** and **2b**, containing sulfonamide linkage. The desired products were explicitly characterized by NMR spectra (^{1}H NMR, ^{13}C NMR), IR and Mass spectrum (Figs. S1 – S6).

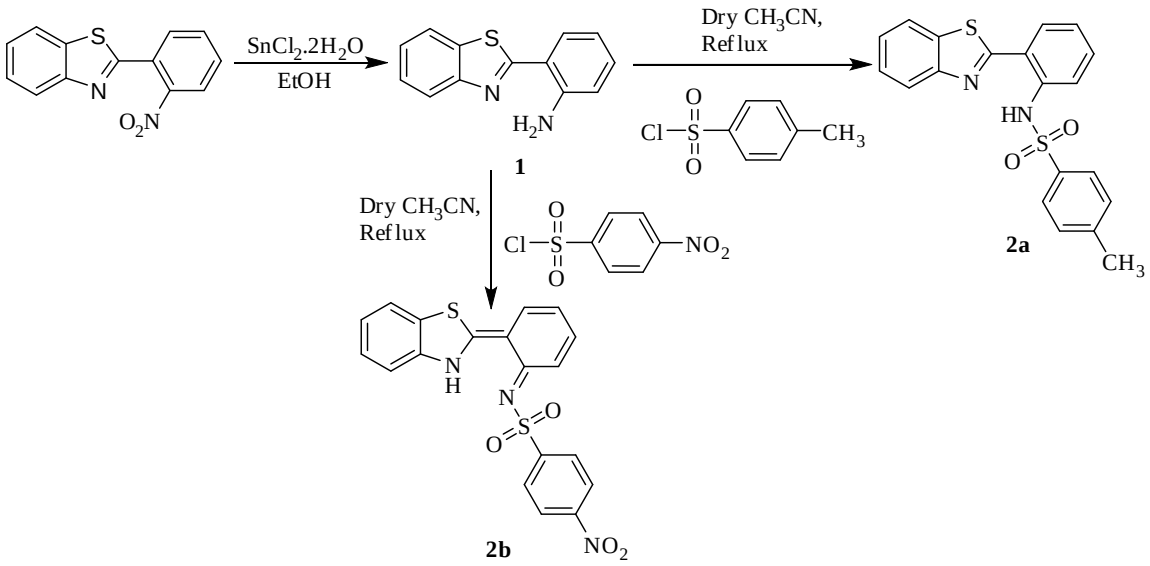

Scheme 1. Synthetic procedure for receptors **2a** and **2b**.

4.1 UV-Vis spectral studies of receptors 2a and 2b

The metal ion binding affinity of **2a** (30 μM) was determined by both UV-Vis absorption spectra and fluorescence emission spectra in the absence and presence of various cations such as Na^+, K^+, Mg^{2+}, Al^{3+}, Ni^{2+}, Cu^{2+}, Fe^{2+}, Fe^{3+}, Zn^{2+}, Cd^{2+}, Hg^{2+}, Co^{2+}, Pb^{2+} (as their perchlorate salts) and anions such as AcO^-, F^-, Cl^-, Br^-, I^-, $H_2PO_4^-$, and HSO_4^- (as their tetrabutylammonium salts), in CH_3CN. In the absence of mentioned ions, the UV-Vis absorption spectrum of **2a** showed two characteristic absorption maxima λ_{max} at 294 nm and 324 nm (Fig. 1). The low energy band (324 nm) was anticipated to intramolecular charge transfer (ICT) transition while the second high energy band at 294 nm corresponds to $\pi \rightarrow \pi^*$ electronic transitions. The addition of 100 equiv. of Na^+, K^+, Mg^{2+}, Al^{3+}, Ni^{2+}, Cu^{2+}, Fe^{2+}, Fe^{3+}, Cd^{2+}, Hg^{2+}, Co^{2+}, Cl^-, Br^-, I^- and HSO_4^- did not result in any color or spectrum changes (Fig. S7). Addition of 100 equiv. of Pb^{2+} resulted in the precipitation of the solution. The increased absorbance due to Cu^{2+} ions at 294 and 324 nm was due to their own absorbance near 300 nm (Fig. S8) and for the same reason, any actual changes observed with Cu^{2+} cannot be identified. However, it was observed that upon addition of F^- and AcO^- ions, receptor **2a** resulted in dramatic absorption changes.

Upon addition of F^- to **2a**, the absorption band at 324 nm reduced gradually and new band appeared at 378 nm, with concomitant development of an isosbestic point at 348 nm. The formation of isosbestic point showed the presence of two ionic species in the medium. This new band appeared with considerable red shift of 54 nm may be attributed to increased

intramolecular charge transfer (ICT) transition within the whole molecule arising due to F^- ion binding (Fig. 1) [28].

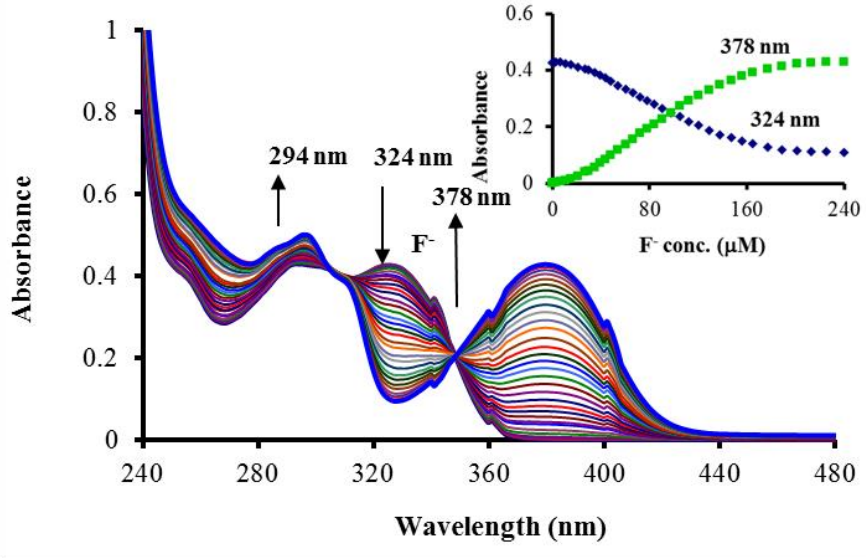

Fig. 1. Family of UV-Vis spectra taken in the course of the titration of **2a** (30 μM in CH_3CN) with F^- ions; Inset: Plot of absorbances at 324 and 378 nm vs. the concentration of F^- added.

Similar type of absorption changes i.e. decreased absorbance at 324 nm and emergence of new band at 378 nm, were observed with addition of AcO^- ions to CH_3CN solution of **2a** (Fig. S9). To know the stoichiometry between the guest (F^- /AcO^-) and host (**2a**) in CH_3CN solution, Job's plot (Fig. S10) has been drawn that showed 1:1 stoichiometry. The association constants of **2a** with F^- and AcO^- were calculated based on the UV-Vis titration through the Benesi-Hildebrand equation [29-30] and found to be 7.20 x 10^6 M^{-1} (LOD=4.7 μM) and 1.5 x 10^5 M^{-1} (LOD=5 μM), respectively.

The UV-Vis spectrum of other receptor **2b** possessing $–NO_2$ group did not show changes upon addition of any of cations and anions (Fig. S11).

4.2 Fluorescence spectral studies of receptors 2a and 2b

4.2.1 Metal ion sensing properties

When excited at 340 nm, **2a** which contains an intramolecular hydrogen bond, underwent ESIPT and yielded a highly stoke's shifted low-intensity emission at 551 nm. As depicted in Fig. 2, among 100 equiv. of various metal ions such as Na^+, K^+, Mg^{2+}, Al^{3+}, Mn^{2+}, Fe^{2+}, Fe^{3+}, Co^{2+}, Ni^{2+}, Cu^{2+}, Zn^{2+}, Cd^{2+} and Hg^{2+} and Pb^{2+}, only Zn^{2+} yielded a bright, blue-shifted fluorescence emission when added to a CH_3CN solution of **2a** (5 μM; λ_{ex} 340 nm). Addition of 100 equiv. of Pb^{2+} resulted in the precipitation of the solution. Recently, Badiei et al synthesized benzimidazole based chemosensor that showed a quenched red-shifted fluorescent peak in the presence of Zn^{2+} ion [31]. However, its -NO_2 analogue, **2b**, was weakly fluorescent and thus, effect of addition of cations and anions cannot be studied [32].

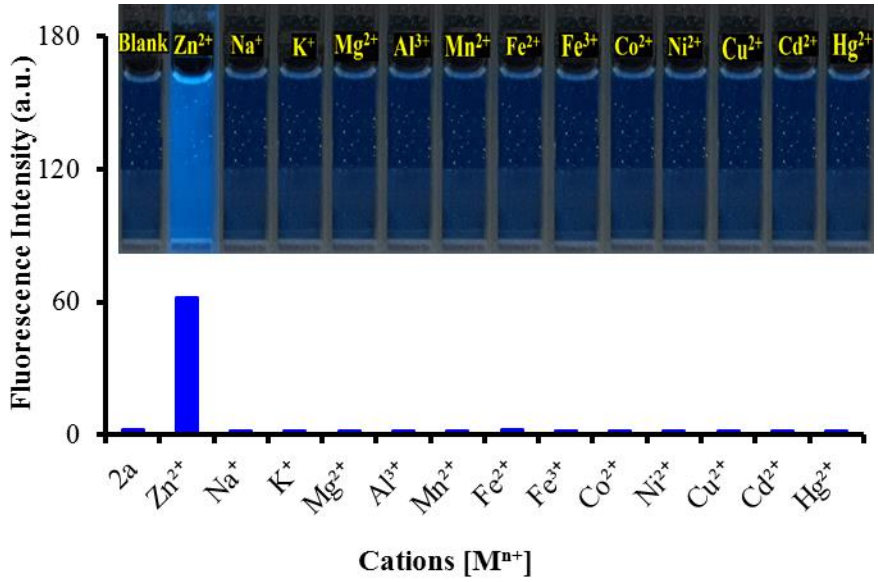

Fig. 2. Fluorescence response of **2a** (5 µM) to various metal ions (500 µM) in CH_3CN. Bars represent the fluorescence inetnsity at 456 nm. Inset: Fluorescence color change observed upon addition of various metal ions.

In the fluorescence titration spectra of **2a** (Fig. 3), at the initial stage of Zn^{2+} addition (0-0.2 equiv.) emission band at 551 nm underwent a hypsochromic shift to 456 nm gradually. This was ascribed as the Zn^{2+} coordinated with sulfonamide and benzothiazole groups and disrupted the ESIPT, thus causing emission with a normal Stoke's shift. On further addition of Zn^{2+} (0.2-40 equiv.) this new emission band underwent fluorescent enhancement around 456 nm. The binding mode of **2a** with Zn^{2+} from the results of fluorescence titration spectra and Job's plot (Fig. S12) showed to be 1:1 with binding affinity (K_a) of 2.4 x 10^4 M^{-1} (LOD=9.7 µM).

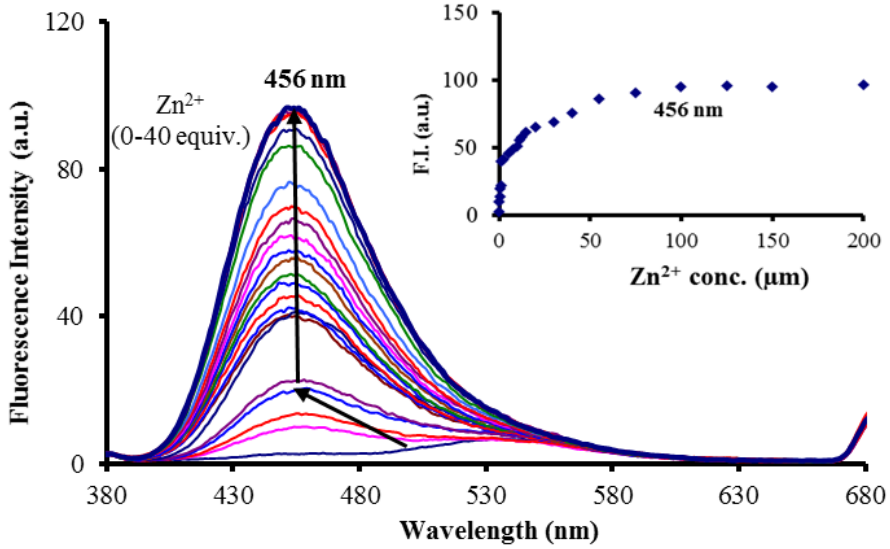

Fig. 3. Family of fluorescence spectra taken in the course of the titration of **2a** (5 µM in CH_3CN; λ_{ex} 340 nm) with Zn^{2+} ions; Inset: Plot of absorbances at 456 nm vs. the concentration of Zn^{2+} added.

The selectivity and tolerance of **2a** for Zn^{2+} ion over other metal cations such as Na^{+}, K^{+}, Mg^{2+}, Mn^{2+}, Fe^{2+}, Co^{2+}, Ni^{2+}, Cu^{2+}, and Cd^{2+} were investigated. The hypsochromic shift and fluorescent enhancement induced by Zn^{2+} remained almost unperturbed and did not get any interference by the coexistence of other interfering cations (Fig. 4a). Earlier literature reports also point to the selectivity of chemosensors towards Zn2+ ions in presence of other interfering cations such as Ni^{2+} and Co^{2+} [33-35]. However, upon addition of more than two times of other metal ions, the paramagnetic transition-metal cations Fe^{2+}, Fe^{3+} and Cu^{2+} partially or completely quenched the fluorescence emission due to non-radiative decay of the excited states [36]. Also addition of excess of Hg^{2+} ions quenched the fluorescence due to heavy atom effect.

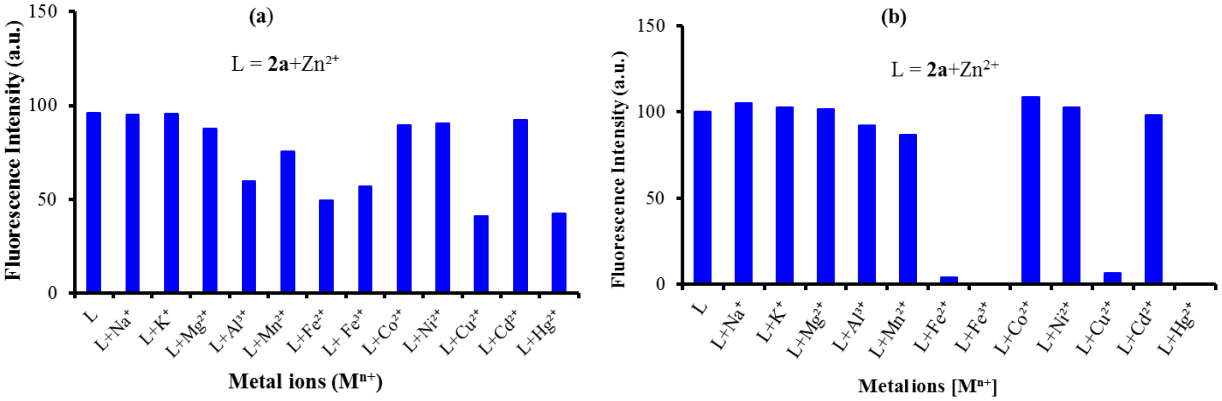

Fig. 4. Metal ion selectivity profile of **2a** (5 µM) via changes observed in fluorescence emission spectra with addition of 40 equiv. of Zn^{2+} with (a) 40 equiv. and (b) 100 equiv. of other interfering cations.

4.2.2 Anion sensing properties

The qualitative anion sensing behavior of **2a** (5 µM) was determined by recording the fluorescence spectra in CH_3CN (λ_{ex} 340 nm). The low intensity emission band was observed at 551 nm. Upon interaction with F^{-}, AcO^{-} and $H_2PO_4^{-}$ ions, enhancement of fluorescence intensity has been observed at 468 nm. In the case of weak basic ions such as Cl^{-}, Br^{-}, I^{-} and HSO_4^{-}, ClO_4^{-} only nominal changes were observed in the fluorescence spectra (Fig. 5).

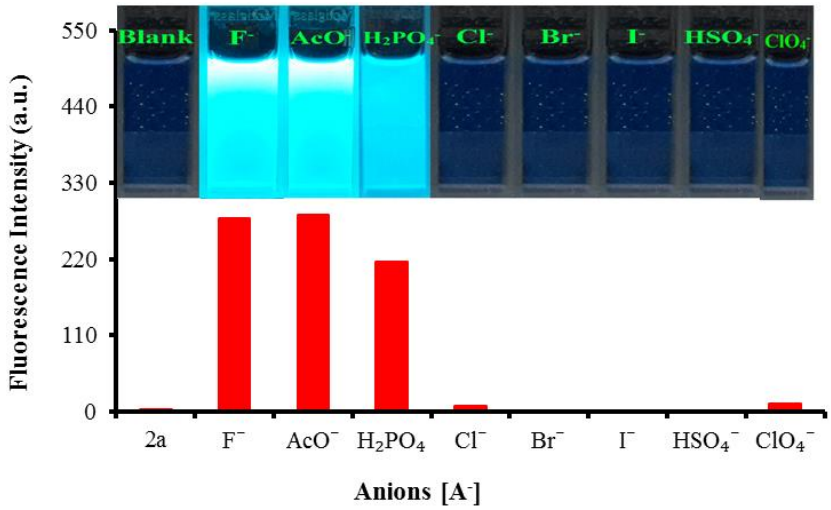

Fig. 5. Fluorescence response of **2a** (5 μM) to various anions (500 μM) in CH_3CN. Bars represent the fluorescence intensity at 468 nm. Inset: Fluorescence color change observed upon addition of various anions.

Fluorescence titrations were next carried out with increasing concentrations of F^-, AcO^- and $H_2PO_4^-$ anions. Upon gradual addition of F^- (0-20 equiv.) to solution of **2a**, the low-intensity tautomeric emission band (λ_{em} 551 nm) underwent hypsochromic shift (λ_{em} 468 nm), along with a great fluorescence enhancement induced by the deprotonation (Fig. 6). This fluorescence enhancement was accompanied by color change from dark blue to light blue, when irradiated with light of wavelength 365 nm (Fig. 5 inset).

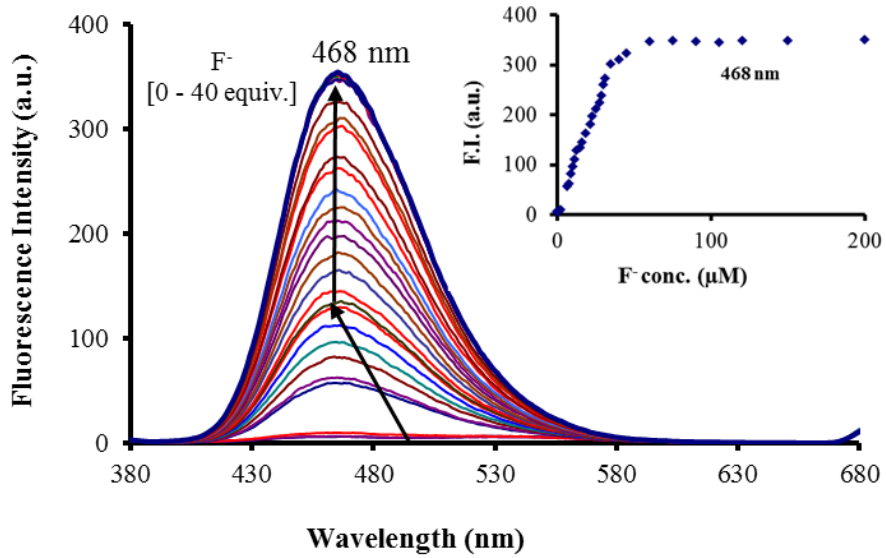

Fig. 6. Family of fluorescence spectra taken in the course of the titration of **2a** (5 μM in CH_3CN; λ_{ex} 340 nm) with F^- ions; Inset: Plot of fluorescence intensity at 468 nm vs. the concentration of F^- added.

Similar effects were observed in the fluorescence spectra of **2a** upon the addition of AcO^- and $H_2PO_4^-$ ions (Fig. S13-S14). Addition of these two ions also resulted in appearance of new blue shifted band at 468 nm. Thus, addition of more basic anions might have induced

deprotonation of sulfonamide proton, which was earlier responsible for causing ESIPT phenomenon. Consequently, the fluorescence anion titrations experienced the disappearance of the tautomer emission (λ_{em} 551 nm) in favor of the deprotonation emission (λ_{em} 468 nm). For F^-, AcO^- and $H_2PO_4^-$ titrations, Job's plot gave 1:1 stoichiometry (Fig. S14), for which binding constants were found to be in order of 9.4 x 10^6 M^{-1} (LOD=2.9 µM), 2.1 x 10^5 M^{-1} (LOD=16 µM) and 9.6 x 10^4 M^{-1} (LOD=20 µM), respectively.

The selectivity of **2a** for $F^-/AcO^-/H_2PO_4^-$ ions over other anions such as Cl^-, Br^-, I^- and HSO_4^-, ClO_4^- were investigated by taking 30 equiv. of $F^-/AcO^-/H_2PO_4^-$ and 30 equiv. of other interfering anions. (Fig. 7).The anions induced hypsochromic shift and fluorescent enhancement remained unperturbed and did not get any interference by the coexistence of other interfering anions (Fig. 7).

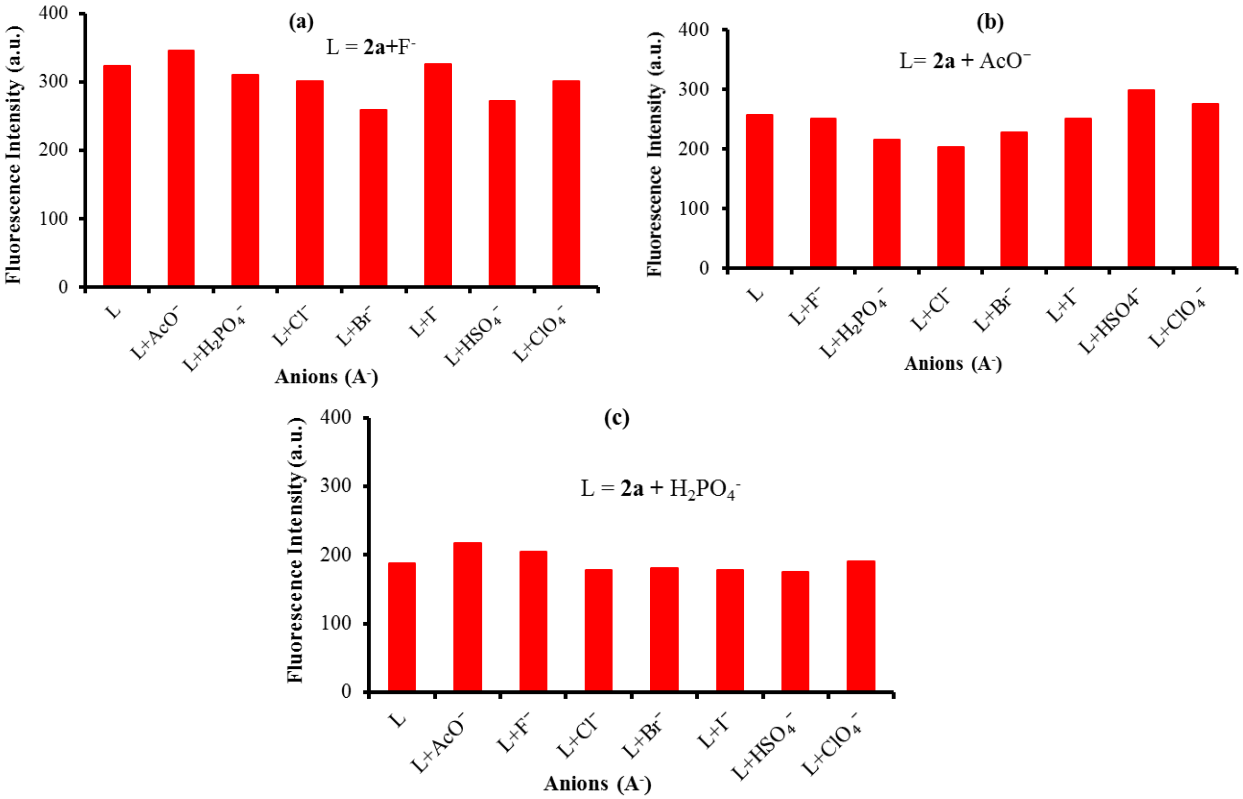

Fig. 7. Anion selectivity profile of **2a** (5 µM) via changes observed in fluorescence emission spectra with addition of 30 equiv. of (a) F^-; (b) AcO^- and (c) $H_2PO_4^-$ ions in the presence of 30 equiv. of other interfering anions.

4.3 ^{1}H NMR titrations

To further elucidate the nature of the intermolecular interactions between anions and receptor **2a**, ^{1}H NMR titration experiments of **2a** (3 x 10^{-2} mol l^{-1}) with F^- were performed in DMSO-d_6. The systematic alterations in ^{1}H NMR signals of **2a** upon addition of progressive amount of F^- ion have been depicted in Fig. 8. The hydrogen bond interaction (deprotonation in

extreme cases) between the binding sites of the host and the anion may give rise to two effects: (i) through-bond effects which results in the upfield shifting of protons in ^{1}H NMR spectrum due to increased electron density of the benzene ring and (ii) through-space effects, which, polarize C–H bond in proximity to hydrogen bond, create the partial positive charge on the proton and cause downfield shifts [37]. In Fig. 8, the NH of receptor **2a** appeared as sharp singlet at δ 11.8. Addition of 0.5 equiv. of F^- broadened this signal and finally, NH signal disappeared after addition of 1.0 equiv. of F^- ions. Moreover, all the aromatic protons shifted upfield, indicative of the increase in the electron density of the phenyl ring owing to the through-bond effects. This increased electron density caused the remarkable bathochromic shift in UV-Vis and emission enhancement in fluorescence spectra of the **2a**.

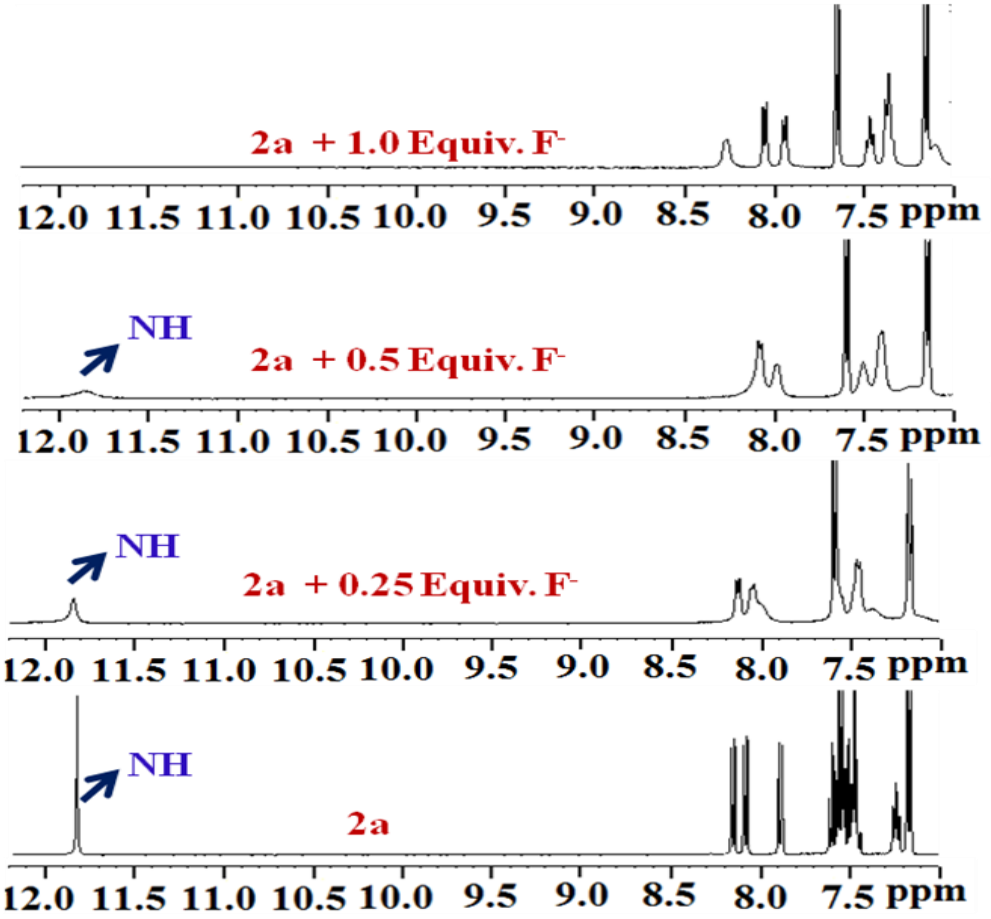

Fig. 8. Partial ^{1}H NMR titration spectra of **2a** (3.0 x 10^{-2} M) upon increasing addition of F^- (TBA^+F^-) ion (0 – 1 Equiv.) in DMSO-d6.

4.4 Plausible sensing model

In CH_3CN, **2a** existed in its tautomeric form displaying weak emission at 551 nm. The addition of F^-, AcO^- and $H_2PO_4^-$ inhibited the intramolecular proton transfer from sulfonamide NH to benzothiazole nitrogen and caused the intermolecular proton transfer from sulfonamide NH to F^-, which has been shown by the ^{1}H NMR titration. As

electronegativity of fluoride is greater compared to nitrogen as well as strong hydrogen bond interaction of fluoride with sulfonamide NH rather than benzothiazole nitrogen, there is more stabilization of negative charge on F^- ion compared to the negative charge on benzothiazole nitrogen, which made the probability of proton transfer to benzothiazole nitrogen comparatively less. The same type of intramolecular proton transfer has been shown by Aslan et al recently [38]. Moreover, emission enhancement observed in fluorescence spectra of **2a** upon addition of Zn^{2+} might be attributed to the inhibition of ESIPT phenomenon, which favored the intramolecular charge transfer (ICT) transition within the whole molecule (Scheme 2).

On the other hand, ^{1}H NMR spectrum of **2b** revealed that NH proton appeared at much upfield value i.e. at δ 7.21 in comparison to that of **2a** which showed NH proton at δ 11.8. This implied that sulfonamide proton completely moved to the benzothiazole moiety in the **2b**, making it less acidic to bind with any of anions.

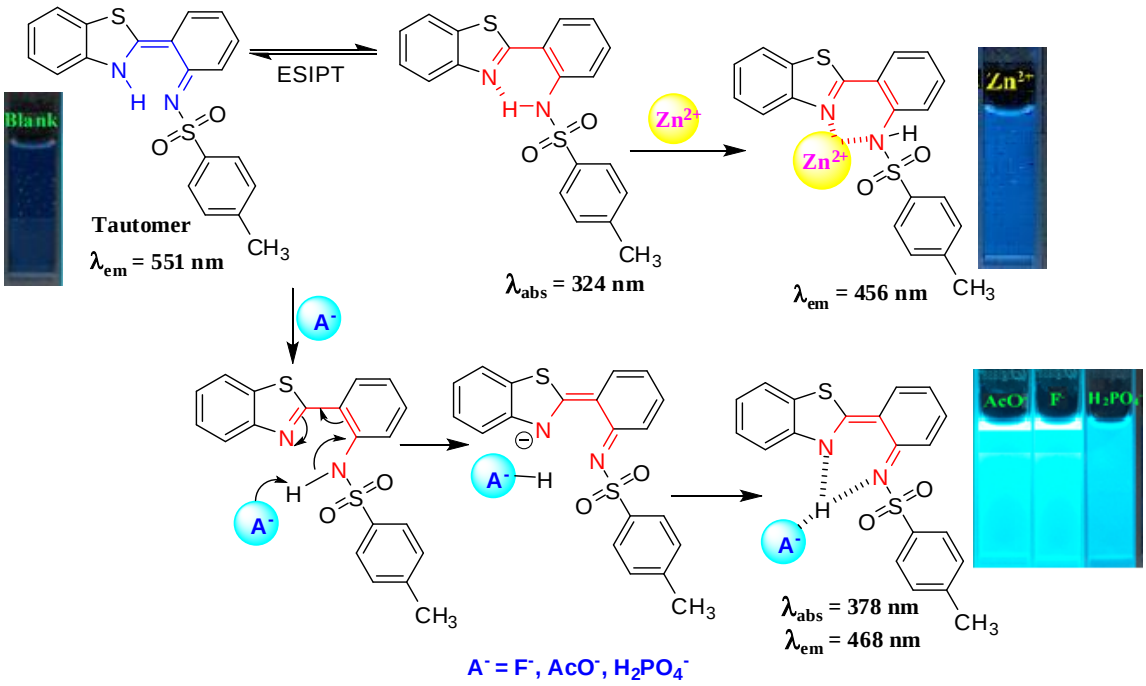

Scheme 2. Possible sensing mechanism of **2a** with analytes in the ground and excited states in CH_3CN.

Conclusions

To sum up, condensation of 2-(2'-aminophenyl)benzothiazole with p-toluenesulfonyl chloride yielded **2a** that has been utilized to detect Zn^{2+} selectively amongst various interfering cations in CH_3CN solvent. Addition of F^-, AcO^- and $H_2PO_4^-$ to solution of **2a** resulted in formation of new band at longer wavength ($\Delta\lambda$ = 54 nm) in UV-Vis spectra and substantial blue shift ($\Delta\lambda$ = 83 nm) along with fluorescent enhancement in fluorescence

spectra. These changes could be attributed to the inhibition of excited state intramolecular proton transfer (ESIPT) due to deprotonation of sulfonamide proton in the presence of F^-, AcO^- and $H_2PO_4^-$ ions.

Acknowledgements

The authors are greatly thankful to SAIF, Panjab University Chandigarh for recording the NMR and Mass spectra and are grateful to DST (Grant no. SR/FT/CS-36/2011), UGC (Grant no. AB2/12/3115) and DST PURSE-II (Grant no. 48/RPC) for the financial assistance.

References

[1] Z. Xu, X. Qian, J. Cui, R. Zhang, Tetrahedron 62 (2006) 10117.

[2] J. S. Kim, D. T. Quang, Chem. Rev. 107 (2007) 3780.

[3] H. N. Kim, M. H. Lee, H. J. Kim, J. S. Kim, Chem. Soc. Rev. 37 (2008) 1465.

[4] A. Helal, H.-S. Kim, Tetrahdron Lett. 50 (2009) 5510.

[5] S. C. Burdette, S. J. Lippard, Proc. Natl. Acad. Sci. U.S.A. 100 (2003) 3605.

[6] A. B. Chausmer, J. Am. Coll. Nutr. 17 (1998) 109.

[7] C. J. Frederickson, J. Y. Koh, A. I. Bush, Nat. Rev. Neurosci. 6 (2005) 449.

[8] M. P. Cuajungco, G. J. Lees, Neurobiol. Dis. 4 (1997) 137.

[9] A. Helal, H.-S. Kim, Tetrahedron 66 (2010) 7097.

[10] C. Caltagirone, P. A. Gale, Chem. Soc. Rev. 38 (2009) 520.

[11] D. Voet, J. G. Voet, Biochemistry 2nd ed., wiley, New York, NY, 1995, 785.

[12] T. Hirano, K. Kikuchi, Y. Urano, T. Nagano, J. Am. Chem. Soc. 124 (2002) 6555.

[13] Y. Mikata, A. Yamanaka, A. Yamashita, S. Yano, Inorg. Chem. 47 (2008) 7295.

[14] K. Hanaoka, K. Kikuchi, H. Kojima, Y. Urano, T. Nagano, J. Am. Chem. Soc. 126 (2004) 12470.

[15] K. Komatsu, Y. Urano, H. Kojima, T. Nagano, J. Am. Chem. Soc. 129 (2007) 13447.

[16] M. Taki, Y. Watanabe, Y. Yukio, Tetrahedron Lett. 50 (2009) 1345.

[17] T. H. Evers, M. A. M. Appelhof, E. W. Meijer, M. Merkx, Protein Eng. Des. Sel. 21 (2008) 529.

[18] D. Bansal, R. Gupta, Dalton Trans. 45 (2016) 502.

[19] G. Grynkiewicz, M. Poenie, R. Y. Tsien, J. Biol. Chem. 260 (1985) 3440.

[20] M. Taki, J. L. Wolford, T. V. O'Halloran, J. Am. Chem. Soc. 126 (2004) 712.

[21] M. M. Henary, Y. G. Wu, C. J. Fahrni, Chem. Eur. J. 10 (2004) 3015.

[22] Y. Wu, J. Fan, S. Gao, M. Tian, J. Zhao, S. Sun, X. Peng, J. Org. Chem. 72 (2007) 62.

[23] G. Zhou, Y. X. Chang, L. X. Wang, X. B. Jing, F. S. Wang, Macromolecules 38 (2005) 2148.

[24] A. Helal, N. T. T. Thao, S. Lee, H.-S. Kim, J. Inclusion Phenom. Macrocycl. Chem. 66 (2010) 87.

[25] A. Helal, S. H. Lee, S. H. Kim, H.-S. Kim, Tetrahedron Lett. 51 (2010) 3531.

[26] A. Helal, H.-S. Kim, Tetrahdron 66 (2010) 9925.

[27] F. D. Bellamy, K. Ou, Tetrahedron Lett. 25 (1984) 839.

[28] V. Bojinov, N. Georgiev, J. Univ. Chem. Technol. Metall. 46 (2011) 3.

[29] H. A. Benesi, J. H. Hildebrand, J. Am. Chem. Soc. 71 (1949) 2703.

[30] K. A. Connors, Binding constants: The measurement of molecuar complex stability, New York, Wiley 1987.

[31] B. V. Razavi, A. Badiei, N. Lashgari, G. M. Ziarani, J. Fluoresc. 26 (2016) 1723.

[32] X. Yang, X. Gong, Y. Li, Z. Liu, B. Gao, G. Zhang, Y. Cui, G. Sun, G. Zhang, Tetrahedron, 71 (2015) 5069.

[33] X. Qian, J. Wang, Y. Xiao, Z. Zhang, Y. Yang, Q. Xu, J. Mater. Chem. 15 (2005) 2836.

[34] H.-S. Kim, A. Helal, Tetrahedron Lett. 50 (2009) 5510.

[35] Y. Huan, Y. Liu, Q. Fei, H. Shan, M. Cui, Q. Liu, G. Feng, Analyst 139 (2014) 1868.

[36] H. Li, S. Gao, Z. Xi, Inorg. Chem. Commun. 12 (2009) 300.

[37] M. Bonizzoni, L. Fabbrizzi, A. Taglietti, F. Tiengo, Eur. J. Org. Chem. 16 (2006) 3567.

[38] K. Aslan, B. Barare, M. Yildiz, H. Unver, Tetrahedron Lett. 57 (2016) 537.